

# Wet Deposition of Persistent Organic Pollutants to the Global Oceans

ELENA JURADO,<sup>†</sup> FODAY JAWARD,<sup>‡</sup>  
RAINER LOHMANN,<sup>\*,§</sup> KEVIN C. JONES,<sup>‡</sup>  
RAFAEL SIMÓ,<sup>||</sup> AND JORDI DACHS<sup>\*,†</sup>

Department of Environmental Chemistry, IIQAB-CSIC,  
Jordi Girona 18-26, Barcelona 08034, Catalunya, Spain,  
Environmental Science Department, Lancaster University,  
Lancaster, LA1 4YQ, U.K., and Marine Sciences Institute,  
CMIMA-CSIC, Passeig Marítim de la Barceloneta 37-49,  
Barcelona 08003, Catalunya, Spain

Wet deposition fluxes of polychlorinated biphenyls and polychlorinated dibenzo-*p*-dioxins and furans to the Atlantic Ocean have been estimated by combining meteorological satellite data and measured atmospheric field concentrations. They are then compared to other atmospheric depositional mechanisms on a global scale. Additional features not treated in traditional studies are addressed such as contaminant adsorption onto raindrops and enhancement of dry gaseous diffusive fluxes due to rain-induced turbulence. Wet deposition estimates show a high spatial and seasonal variability, with maxima located in the Intertropical Convergence Zone (ITCZ) and in low-temperature regions. Seasonal variability reflects the northward shift of ITCZ in July. Average wet deposition fluxes estimated for the Atlantic Ocean in this study are 110 and 45 ng m<sup>-2</sup> yr<sup>-1</sup> for ΣPCB and ΣPCDD/Fs, respectively. Furthermore, the total wet deposition to the Atlantic results in 4100 kg yr<sup>-1</sup> (ΣPCB) and 2500 kg yr<sup>-1</sup> (ΣPCDD/Fs). Model validation shows good agreement with available coastal data measurements of wet deposition fluxes. When compared to other atmospheric depositional mechanisms and during precipitation events, wet deposition is found to be dominant. However, when raining events and non-raining time periods are integrated, air–water diffusive exchange fluxes acquire an important role, which can be dominant in some regions and for some POPs.

## Introduction

Persistent organic pollutants (POPs) are transported long distances from source regions to remote regions through atmospheric transport and deposition (1–3). Subsequently, deposition of POPs may be the major process by which they impact remote oceanic areas, raising environmental concerns because of their toxicity and accumulation in aquatic food webs (4, 5). Furthermore, the oceans account for a significant global sink of POPs (6, 7).

Since POPs are semivolatile compounds, they occur both in the gas and aerosol phases (8); thus precipitation scavenging will deposit POPs in dissolved and particulate forms (9). Available measurements of POP wet deposition fluxes in oceanic regions are very scarce, even though they are needed because of the key role of oceanic controls on regional and global dynamics and sinks of POPs (7). Given the important seasonal and spatial variability of precipitation rates, spatially resolved estimates of wet deposition fluxes at the global scale are required. In this context, climatological parameters retrieved with remote sensing instruments can provide very useful data, an area that has been developed intensively for the last 30 yr. Satellites provide two parameters useful in environmental models; precipitation rate ( $p_0$ , mm month<sup>-1</sup>) and the fraction of the time that it is actually raining ( $f$ , dimensionless).

Apart from wet deposition, deposition of POPs can occur as dry gaseous, or air–water exchange, and dry particulate forms. The relative importance of wet deposition fluxes versus other depositional processes is still in debate. Previous studies have shown that diffusive gaseous air–water exchange dominates over wet and dry particle deposition of POPs, except in rainy regions and close to urban areas with a high concentration of atmospheric particulate matter and for chemicals that have a strong affinity to aerosols such as polycyclic aromatic hydrocarbons (PAHs) (10, 11). However, the studies that compare different depositional mechanisms estimate air–sea fluxes using correlations derived during non-raining periods. Recently, it has been shown that turbulence generated by rain droplets enhances the diffusive fluxes of some tracers (12, 13), but the significance of this process for POPs has not yet been assessed.

The objectives of this study are as follows: (i) To develop a methodology to estimate the spatial and temporal variability of wet deposition fluxes of POPs over the Atlantic, inferred from satellite data and atmospheric field measurements of gas and aerosol-phase POP. Additional features such as the adsorption of the contaminant to the surface of the raindrop (14) have been addressed. (ii) To compare on a global scale spatially resolved wet deposition fluxes to other depositional processes, such as diffusive air–water exchange, enhanced by rain droplets-induced turbulence, and dry aerosol deposition. This study is a companion paper of a recent study of dry aerosol deposition fluxes of POPs to the global oceans (15).

## Field Measurements and Data Sources

**Atmospheric Concentration Data.** This work is based on atmospheric ship-board air concentrations of two representative families of POPs, polychlorinated dibenzo-*p*-dioxins and furans (PCDD/Fs) and polychlorinated biphenyls (PCBs), obtained during two north–south Atlantic Ocean transects. Air samples of PCDD/Fs were taken onboard the RRS *Bransfield*, during an Atlantic cruise from the U.K. to Antarctica in October–December 1998 (52°N, 1°E–75°S, 20°W) (16). PCBs were analyzed in samples obtained between The Netherlands and South Africa in January–February 2001 onboard the R/V *Pelagia* (52°N, 1°E–34°S, 20°E) (17). Gas- and aerosol-phase POP concentrations were obtained from high-volume samplers. In the case of PCBs, only gas-phase concentrations were determined since PCB concentrations in the aerosol phase were below the detection limit. Latitudinal profiles of PCDD/Fs show an important variability with higher values at low latitudes than at mid-high latitudes, except in areas close to urban regions. Details of the methods and data variability and trends can be found elsewhere (16,

\* Corresponding author phone: +34-93-400-6100; e-mail: jdmqam@cid.csic.es.

<sup>†</sup> IIQAB-CSIC.

<sup>‡</sup> Lancaster University.

<sup>§</sup> Present address: Graduate School of Oceanography, University of Rhode Island, Narragansett, RI 02882-1197.

<sup>||</sup> CMIMA-CSIC.

17). POP dissolved water concentrations were estimated by applying the phytoplankton uptake and sinking model developed by Dachs et al. (18). This parameterization has been successfully applied in previous studies (19, 20).

**Satellite Data.** Meteorological input data for modeling has been retrieved from remote sensing measurements. Sea surface temperatures (SST) were obtained from the Along Track Scanning Radiometer (ATSR) installed in the European Space Agency ERS-2 satellite (ATSR project web page <http://www.atsr.rl.ac.uk/>). SST images consist of monthly averaged data with a resolution of  $0.5^\circ$  and an accuracy of  $\pm 0.3$  K. Monthly global wind speed distributions ( $u_{10}$ ), referred to 10 m above the surface of the sea, were obtained from the NOAA special sensor microwave/imager (SSM/I) at a resolution of  $1^\circ \times 1^\circ$  and an accuracy  $\pm 2$  m s $^{-1}$  (<http://lwf.ncdc.noaa.gov/oa/satellite/ssmi>).

Precipitation data, namely, monthly rainfall rate ( $p_0$ ) and the fractional occurrence of precipitation ( $f$ ), were also obtained from SSM/I NOAA. Determination of rainfall by passive microwave sensors, such as SSM/I, may be underestimated during low rainfall periods and overestimated during wet periods, leading to some inaccuracies in the tropics. However, rainfall retrieval over the ocean from SSM/I represents the best compromise between estimation accuracy and spatial data coverage (21). Uncertainty is about 15–30% when compared to rain gauge data sets (22).

Aerosol derived parameters (size distribution, mass concentration) were obtained from the Moderate-Resolution Imaging Spectrometer Instrument (MODIS, <http://modis.gsfc.nasa.gov/>) and by applying conversion factors as described in a companion paper (15). The used data set correspond to monthly mean values in the period of field sampling (either November 1998 or January 2001). Since MODIS remote sensing parameters for aerosol data were not available before 2001, climatological means for November and January of two consecutive years (2002, 2003) have been used (15).

## Model Development

**Estimation of Wet Deposition Flux.** The wet deposition flux ( $F_{WD}$ , pg m $^{-2}$  d $^{-1}$ ) is given by the product of  $p_0$  and the concentration of the chemical in rain ( $C_R$ , pg m $^{-3}$ ), which includes both the dissolved and particulate phases:

$$F_{WD} = p_0 C_R \quad (1)$$

Here,  $p_0$  (m d $^{-1}$ ) is the precipitation depth per day, derived from satellite values of monthly mean. Since  $C_R$  is unknown, an empirical approach has been applied that makes use of an overall scavenging ratio ( $W_T$ , dimensionless), which is the ratio of concentrations in rain and in the atmosphere ( $C_A$ , pg m $^{-3}$ ), the latter including gas-phase ( $C_G$ , pg m $^{-3}$ ) and aerosol-phase concentrations ( $C_P$ , pg m $^{-3}$ ).

$W_T$ , also termed overall washout ratio, can alternatively be estimated by (9, 23)

$$W_T = W_G(1 - \phi) + W_P(\phi) \quad (2)$$

in which  $W_G$  and  $W_P$  are the gas and particle washout ratios, respectively; and  $\phi$  (dimensionless) is the fraction of aerosol-bound POPs to total atmospheric POP concentration ( $C_P / (C_P + C_G)$ ).  $\phi$  values for PCDD/F are determined using measured field  $C_G$  and  $C_P$  concentrations, while for PCBs it has been necessary to estimate it from gas-particle partitioning models (8) by

$$\phi = \frac{K_p(\text{TSP})}{1 + K_p(\text{TSP})} \quad (3)$$

Details of the derivation of the particle–gas partition coefficient ( $K_p$ , m $^3$  kg $^{-1}$ ) and TSP (the total suspended particle matter, kg m $^{-3}$ ) from physicochemical properties and remote sensing measurements, have been described elsewhere (15, 24–26).

In terms of  $\phi$ ,  $F_{WD}$  can be expressed by

$$F_{WD} = (W_G(1 - \phi) + W_P(\phi))p_0 C_A = \left( W_G + \frac{W_P Q}{(1 - \phi)} \right) p_0 C_G \quad (4)$$

It is important to note that the previous equation accounts for the flux for an average day, which includes raining and non-raining periods. Additionally, it is useful to refer the wet deposition flux just to the time when the precipitation event is occurring (raining period); then the subscript “rain” is added to distinguish from the flux obtained above.  $F_{WD\_rain}$  is given by dividing eq 4 by the fractional occurrence of rain ( $f$ ):

$$F_{WD\_rain} = \left( W_G + \frac{W_P \phi}{(1 - \phi)} \right) \frac{p_0}{f} C_G \quad (5)$$

**Parameterization of Washout Ratios.** Traditionally  $W_G$ , defined as the ratio of the rain-dissolved phase to gas-phase POP concentrations, has been estimated using the Henry's law constant ( $H$ , Pa m $^3$  mol $^{-1}$ ), assuming that equilibrium is attained rapidly between the gas phase and the dissolved phase in a raindrop. However, field-measured gas washout of atmospheric POPs have found to be higher (27–29). A recent study concluded that a better estimation of  $W_G$  is obtained when POP adsorption to the raindrop surface from the gas phase is considered (14). Therefore,  $W_G$  is the sum of the absorption gas-phase washout ( $W_{G\_diss}$ ) and the gas-phase washout due to adsorption on the raindrop ( $W_{G\_ads}$ ):

$$W_G = W_{G\_diss} + W_{G\_ads} \quad (6)$$

$$W_{G\_diss} = \frac{RT}{H} \quad (7)$$

$$W_{G\_ads} = 2000 \times K_{ia} \times \Lambda \quad (8)$$

where  $T$  (K) and  $R$  (8.314 Pa m $^3$  mol $^{-1}$  K $^{-1}$ ) are respectively the temperature and the gas constant;  $K_{ia}$  (m $^3$  m $^{-2}$ ) is the water interface/gas partitioning coefficient, estimated from the subcooled liquid saturated vapor pressure (14, 30); and  $\Lambda = 4.1 \times ((1000p_0/f24))^{-0.21}$  (mm $^{-1}$ ) is a parameter of the exponential law, proposed by Marshall and Palmer (31), for the size distribution of raindrops. The temperature dependence of  $H$  has been estimated as suggested by Brunner et al. (32). There are other data sets of Henry's law constant widely used (33, 34) and sometimes different than those of Brunner et al. (32). The temperature dependence of  $H$  values depends to a certain extent on the data set; thus, this may have some influence on the results obtained as discussed below. Details on the derivations of  $W_{G\_ads}$  and the assumptions of the raindrop size distribution (Marshall–Palmer) are described in Annex I in the Supporting Information. The inclusion of  $W_{G\_ads}$  makes the parameterization of the gaseous removal of POPs by rain subject to the variability of the precipitation rate. This dependence has been observed in various studies (35). Decreasing rainfall intensity increases  $W_{G\_ads}$  because of the resulting increase of surface-to-volume ratio of the raindrop spectrum.

Figure 1 shows the comparison between  $W_G$  derived including the adsorption on the raindrop surface (eq 6), with the one estimated from Henry's law constant (eq 7) for Cl $_5$ -DD and PCB 101 and in the Atlantic Ocean atmosphere.  $W_G$  values are in the range of  $10^4$ – $6 \times 10^4$  for PCDD/Fs and

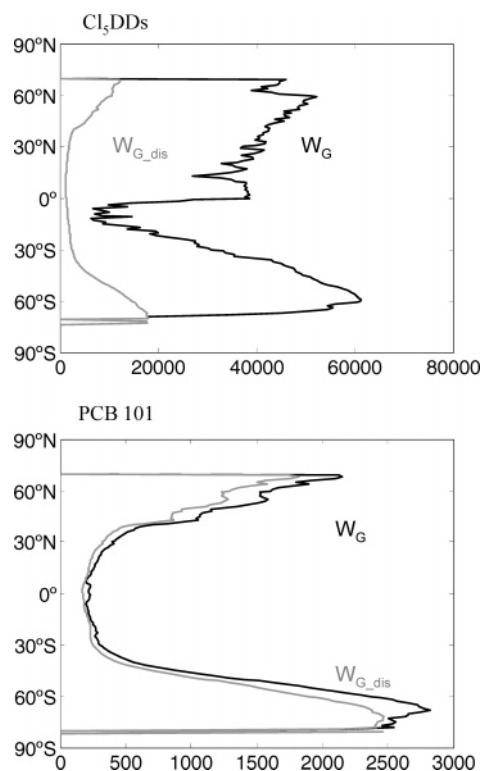


**FIGURE 1.** Comparison between the gas washout considered in this work, taking into account both the adsorption and dissolution on/into the raindrop ( $W_G$ ) or just considering the equilibrium conditions ( $W_{G\_dis}$ ). Latitudinally averaged profiles for the Atlantic Ocean are shown for  $Cl_5DDs$  and PCB 101 are shown.

$5 \times 10^2$ – $3 \times 10^3$  for PCBs. They agree with field measurements such as  $8 \times 10^3$ – $3 \times 10^6$  for PCDD/Fs by Eitzer and Hites (10) in Bloomington, IN (rural area), but overestimates up to an order of magnitude the range of  $2 \times 10$ – $2 \times 10^2$  for PCBs measured by Van Ry et al. (36) in the coastal NW Atlantic

Ocean (Tuckerton, U.S., coastal area). It is seen that the new parameterization (eq 6) has a stronger effect enhancing  $W_G$  for PCDD/Fs than for PCBs. Since it improves the agreement with experimental data (14), the estimations reported here will be those given by eq 6. Gas scavenging efficiency increases with the level of chlorination for both classes of POPs.

Particle scavenging is the process by which rainfall removes aerosols and the compounds bound to those particles from the atmosphere. In contrast to gas scavenging, particle scavenging results not from equilibrium partitioning but rather from complex processes controlled by meteorological conditions and physical–chemical properties of the aerosol. It is inferred that all the compounds bound to aerosols may be affected in a similar way (10). However, some authors such as Franz and Eisenreich (37), Offenberger and Baker (38), and Poster and Baker (29, 39) have measured higher particle washouts for the more volatile POPs. There are very few similar studies, referred to open ocean areas. Reported average measured particle scavenging rates ( $W_P$ ) are highly variable, as seen in Table 1. This can be explained by the complexity of the scavenging process and the natural variability of the aerosol population and meteorological conditions. Theoretically, scavenging rates are expected to increase with particle diameter for supermicron aerosols and decrease with increasing size for submicron aerosols (40), although the exact extent is still not clear (1). Mircea et al. (41) estimated scavenging coefficients that achieved maxima for urban aerosol and minima for marine or continental aerosol, but with almost no dependence on raindrop size distribution. Furthermore, there is no obvious dependence of the particle scavenging rate on the rainfall intensity (42). Provided the reported constraints, an average value of  $2 \times 10^5$  has been adopted, which is consistent with many reported measurements (see Table 1) and has been used in other modeling exercises (43).

**Estimation of Air–Water Diffusive Exchange during Rain Events.** The net diffusive flux ( $F_{AW}$ ,  $pg\ m^{-2}\ d^{-1}$ ) across the air–water interface has been calculated from the mass transfer rate coefficient ( $k_{AW}$ ,  $m\ d^{-1}$ ) and the concentrations

**TABLE 1.** Particle Washout Ratios Reported in the Literature

compound	particle washout $W_p$ (dimensionless)	year of sampling	location	type of environment	source
semivolatile organic compounds	$2 \times 10^3$ – $10^6$				literature review data, Bidleman (9)
PCBs	$1.9 \times 10^5$ – $5.2 \times 10^5$	2000–2001	Crete Island, eastern Mediterranean	marine background	Mandalakis et al. (64)
PCBs	$4 \times 10^4$ – $2 \times 10^6$	2000–2001	Tuckerton, U.S.	coastal, light residential	Van Ry (36)
PCBs	$2 \times 10^5$ – $2 \times 10^7$	1999–2001	Pineland, U.S.	remote forest	Van Ry (36)
PCBs	$8 \times 10^2$ – $8 \times 10^7$ for submicron particles ( $< 1\ \mu m$ ) $7 \times 10$ – $4 \times 10^9$ for large particles ( $> 1\ \mu m$ )	1994–1995	Lake Michigan, U.S.	suburban	Offenberg and Baker (38)
PCBs	$10^3$ – $10^5$	1991–1992	Minnesota, U.S.	suburban	Franz and Eisenreich (37)
PCDD/Fs	$3 \times 10^4$ – $10^5$	2000	Kanto, Japan	urban	Ogura et al. (59)
PCDD/Fs	$2 \times 10^4$ – $10^5$	1990–1991	Indianapolis, U.S.	suburban	Koester and Hites (35)
PCDD/Fs	$10^4$ – $8 \times 10^4$	1986–1989	Bloomington, U.S.	rural	Eitzer and Hites (10)
PAHs	$3 \times 10^2$ – $3 \times 10^8$ submicron $9 \times 10^3$ – $5 \times 10^8$ large	1994–1995	Lake Michigan, U.S.	suburban	Offenberg and Baker (38)
PAHs	$6 \times 10^2$ – $3 \times 10^4$ submicron $3 \times 10^2$ – $12 \times 10^4$ large	1992	Chesapeake Bay, U.S.	rural	Poster and Baker (29)
PAHs	$10^3$ – $10^6$	1991	Chesapeake Bay, U.S.	rural	Dickhut and Gustafson (28)
PAHs	$2 \times 10^2$ – $4 \times 10^4$	1984	Portland, U.S.	residential	Ligoki et al. (23)



in the bulk air and water phases, by applying the classical two-film approach (44). Absorption ( $F_{AW\_abs}$ ,  $\text{pg m}^{-2} \text{d}^{-1}$ ) and volatilization fluxes ( $F_{AW\_vol}$ ,  $\text{pg m}^{-2} \text{d}^{-1}$ ) are computed respectively by

$$F_{AW\_abs} = k_{AW} \frac{C_G}{H'} \quad (9)$$

$$F_{AW\_vol} = k_{AW} C_W \quad (10)$$

where  $C_W$  ( $\text{pg m}^{-3}$ ) is the POP dissolved-phase concentration, and  $H'$  is the dimensionless Henry's law constant.  $F_{AW}$  is given by the difference between the absorption and the volatilization fluxes. It is important to note that Henry's law values are a key parameter and there is a marked variability in reported values that may exert an important influence on estimations as discussed elsewhere (45). The overall mass transfer coefficient ( $k_{AW}$ ,  $\text{m d}^{-1}$ ) comprises resistance to mass transfer in both water ( $k_W$ ,  $\text{m d}^{-1}$ ) and air films ( $k_A$ ,  $\text{m d}^{-1}$ ):

$$\frac{1}{k_{AW}} = \frac{1}{k_W} + \frac{1}{k_A H'} \quad (11)$$

These mass transfer coefficients have been empirically defined based upon field studies using tracers such as  $\text{CO}_2$ ,  $\text{SF}_6$ , and  $\text{O}_2$ . Scaling of  $k_A$  and  $k_W$  to POPs is done in the traditional manner by taking into account the different diffusivities and Schmidt numbers of POPs (44). Wind speed is a key variable to estimate  $k_{AW}$ , and a considerable effort has gone into determining an empirical relationship (46–48). Even if wind speed exhibits a major control on surface turbulence, which controls the kinetics of air–sea exchange, it is not the only factor. For example, rain has been identified recently as an additional parameter that enhances  $k_W$  values. This has been widely studied by Ho et al. (12, 13), who conclude that rainfall on the ocean significantly enhances the rate of air–sea gas exchange due to the turbulence generated by the impact of raindrops on the water surface. By calculating the kinetic energy of simulated rains, under conditions of no wind and for freshwaters, an empirical correlation between the gas transfer velocity and the rainfall rate has been suggested (12). We assume that the combined effect of wind speed and raindrops falling on the ocean surface is a simple addition of the two individual processes, which normalized to a Schmidt number of 600 ( $k_W(600)$ ,  $\text{cm h}^{-1}$ ), corresponding to the value for  $\text{CO}_2$  at 20 °C, results in

$$k_W(600) = 0.061u_{10} + 0.24u_{10}^2 + 0.679\left(\frac{1000p_0}{24}\right) - 0.0015\left(\frac{1000p_0}{24}\right)^2 \quad (12)$$

where  $u_{10}$  ( $\text{m s}^{-1}$ ) is the wind speed 10 m above the surface. The first two terms from left to right account for the effect of wind speed as suggested by Nightingale (47, 48); the latter two terms, account for the effect of the raindrop-generated turbulence. The relation between  $k_W(600)$  and  $k_W$  can be found elsewhere (18).

Since wind speed and precipitation, retrieved from satellite measurements, correspond to monthly averages, it is important to account for the short-term variability and nonlinear influence of those parameters on the mass transfer coefficient. For example, it is well-known that short periods of high wind speed account for most the time-integrated flux (49). The nonlinear influence of wind speed has been accounted by considering an oceanic Weibull distribution of wind speed with a shape parameter of 2 (50). Conversely, precipitation amounts have been modeled by an exponential distribution that depends on the average nonzero precipitation amount

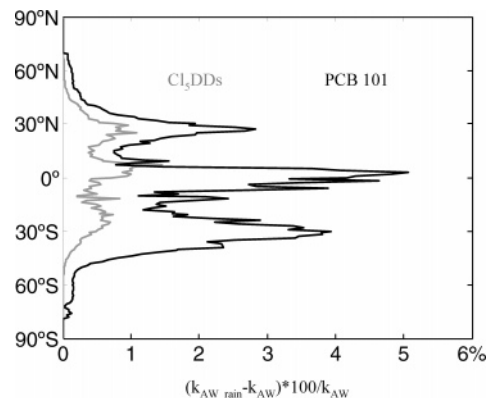


**FIGURE 2.** Increase of the air–water exchange mass transfer coefficient ( $k_{AW}$ ) due to enhanced turbulence generated by rain:  $(k_{AW\_rain} - k_{AW}) \times 100/k_{AW}$ . Values are shown for  $\text{Cl}_2\text{DD}$  and  $\text{PCB 101}$ , latitudinally averaged for the Atlantic Ocean.

( $\mu$ ). The probability density function of the reported exponential distribution is (51)

$$f(x) = \frac{1}{\mu} \exp\left(-\frac{x}{\mu}\right) \quad (13)$$

Therefore, the corresponding expression for the mean  $k_W(600)$  corrected by the nonlinear influence of wind speed and precipitation is given by

$$k_W(600) = 0.061u_{10} + \frac{0.24u_{10}^2 \Gamma(2)}{\Gamma^2(1.5)} + 0.679\left(\frac{1000p_0}{24}\right) - 0.0015\left(\frac{1000p_0}{24}\right)^2 \Gamma(1.5) \quad (14)$$

Where  $\Gamma$  is the gamma function. Figure 2 shows the enhancement of the air–water mass transfer coefficient ( $k_{AW}$ ) due to rain generated turbulences  $((k_{AW\_rain} - k_{AW})/k_{AW})$ . This enhancement does not exceed 10%; maxima are attained in rainy latitudes such as the Intertropical Convergence Zone (ITCZ). This increase in  $k_{AW}$  is smaller than that suggested by Ho's experiments (13, 52). This is mainly due to the moderately high oceanic wind speeds (average  $8 \text{ m s}^{-1}$ ) that overwhelms the influence of precipitation-driven turbulence. However, the latter may still be significant in continental and coastal waters characterized by lower wind speed regimes.

## Results and Discussion

Wet deposition and gross and net air–water exchange fluxes have been estimated using the methodology and field data reported above. The latitudinal profiles of measured gas-phase concentrations (PCDD/Fs and PCBs) and the measured (PCDD/Fs) and predicted (PCBs) aerosol-phase concentrations along the north–south Atlantic cruises have been considered representative of the Atlantic when computing the average depositional fluxes for this ocean.

**Wet Deposition Flux.** The averaged latitudinal profiles of  $F_{WD}$  for the Atlantic Ocean and the contribution of scavenging of aerosol phase POP ( $W_p C_p p_0$ ) to total  $F_{WD}$  are shown in Figure 3. Results are depicted for two characteristic PCDD/Fs ( $\text{Cl}_4\text{DDs}$ ,  $\text{Cl}_7\text{DFs}$ ). Particle scavenging plays a major role, accounting for more than 90% of the total scavenging flux for the higher chlorinated PCDD/Fs. Even though PCBs are found predominantly in the gas phase, particle scavenging also dominates as a removal mechanism during precipitation events, as seen in field studies (38, 53).

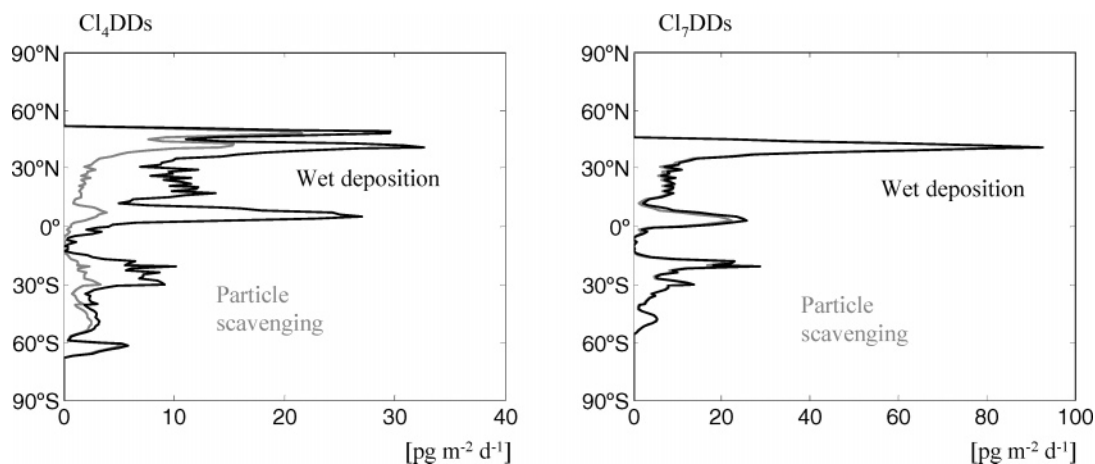


**FIGURE 3.** Latitudinally averaged profiles of the wet deposition flux for  $\text{Cl}_4\text{DDs}$  and  $\text{Cl}_7\text{DFs}$  to the Atlantic Ocean. Wet deposition fluxes due to particle scavenging only are also shown.

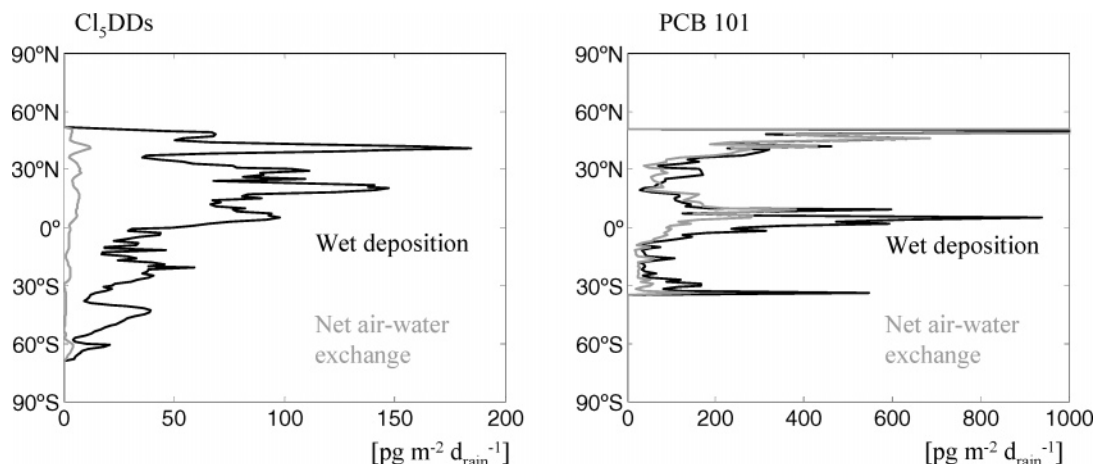


**FIGURE 4.** Latitudinally averaged profiles of the wet deposition and net air–water exchange fluxes for  $\text{Cl}_5\text{DDs}$  and PCB 101 to the Atlantic Ocean. The fluxes are referred to rainy periods.

Additional latitudinal profiles of wet deposition fluxes (and comparison with net air–water exchange fluxes) for other representative PCDD/Fs and PCBs are shown in Figure 4. In contrast to Figure 3, which refer to averaged daily time, these profiles are just for rainy periods (i.e.,  $F_{\text{WD, rain}}$  is shown); thus, greater flux values are observed. The strong spatial variability of wet deposition fluxes is noteworthy. As a general trend observed for all the compounds, the maxima over the Atlantic Ocean are found in the ITCZ, where convective precipitation rates are high. The latitudinal profiles also show the influence of low temperatures, which favor partitioning to aerosols and thus particle scavenging mechanisms, as seen around 50 °N. If an alternative set of Henry's law values are used (33), a different (usually higher) temperature influence on gas scavenging at high latitudes is predicted for some compounds. However, the dependence on the choice of  $H$  values is lower for the total wet deposition fluxes due to the importance of particle scavenging. On the other hand, mid-latitude storm tracks, subtropical high subsidence zones, contribute in mid and high latitudes, resulting in enhanced wet deposition fluxes around 35° S. It is clearly important to consider spatially resolved  $F_{\text{WD}}$  values when assessing atmospheric deposition, and atmospheric residence times on a global scale instead of limiting the study to the mean values.

**Air–Water Exchange Flux during Rainy Periods.** The averaged latitudinal profiles of the net diffusive air–water exchange flux during rainy periods for the Atlantic Ocean are shown in Figure 4. These are shown for a characteristic PCDD/Fs ( $\text{Cl}_5\text{DD}$ ) and PCBs (PCB 101). High PCDD/Fs fluxes

are found in the 0–20° N zone, driven by high gas-phase concentrations in this latitudinal band and meteorological conditions (wind speed and temperature) that favor the air–water exchange of gases. Net fluxes, as described above, are estimated by applying an air–water–phytoplankton exchange model reported elsewhere (18) but with  $k_{\text{AW}}$  estimated as discussed above. Therefore, enhanced sinking fluxes driven by high primary productivity have an important influence on atmospheric gaseous deposition, inducing high fluxes in mid-high latitude areas and in upwelling regions (Off-Sahara, etc). Additionally, PCBs exhibit high levels of diffusive fluxes at the beginning and the end of the cruise, probably caused by higher concentrations from proximate land sources. If gross air–water exchange fluxes are considered, then the magnitude of the flux can become more than 10 times higher as compared to the net amount. This is the case for the majority of the PCBs, highlighting the importance of diffusive exchange as a driver of the atmospheric residence times of POPs.

**Comparison of Atmospheric Depositional Processes to the Atlantic Ocean.** As observed in Figure 4, during a precipitation event, wet deposition is the predominant transport mechanism of pollutants. However, to assess the relative importance of the depositional fluxes in a larger temporal framework, it is necessary to consider wet deposition and net air–water exchange referred as well for the periods without rain and to consider a third depositional mechanism: dry aerosol deposition. Hence, the three depositional fluxes, which will be the basis of the comparison are

$$F_{WD} = \left( W_G + \frac{W_P \phi}{(1 - \phi)} \right) p_0 C_G \quad (15)$$

$$F_{AW} = k_{AW, \text{rain}} \left( \frac{C_G}{H} - C_W \right) f + k_{AW} \left( \frac{C_G}{H} - C_W \right) (1 - f) \quad (16)$$

$$F_{DD} = v_D C_P \quad (17)$$

Details of the derivation of dry deposition velocities ( $v_D$ ,  $\text{m d}^{-1}$ ) from remote sensing measurements are described elsewhere (15). Figure 5 depicts the average of the wet deposition, net air–water exchange, and dry aerosol deposition fluxes for the Atlantic Ocean for all PCDD/Fs and a number of PCB congeners. Values range between 4 and 25  $\text{pg m}^{-2} \text{d}^{-1}$  and between 5 and 100  $\text{pg m}^{-2} \text{d}^{-1}$  for PCDD/Fs and PCBs, respectively. In contrast to Figure 4 that considered rainy periods alone, wet deposition has a more modest role when nonrainy periods are considered. There are also clear differences between the two families of POPs; the wet deposition flux contributes to about 40–75% of the total deposition of PCDD/Fs but in the case of PCBs, it does not represent more than the 35%. PCBs are characterized by important diffusive air–water exchange fluxes that, on average, exceed the rest. Even if dry aerosol deposition represents a minor fraction of the total flux (typically  $\sim 15\%$ ) it can be the dominant mechanism for less volatile PCBs and PCDD/Fs, in areas of high wind speeds and atmospheric particulate concentrations. Wet deposition flux and its contribution to total atmospheric inputs tend to increase with chlorination number, and with decreasing compound volatility, especially for PCB homologues. For PCDD/Fs, gas scavenging makes a higher contribution to the total wet deposition flux due to adsorption to water droplets, resulting in more complex trends with the degree of chlorination. Annex II shows the comparison of wet and dry deposition with the gross air–water exchange fluxes instead of the net fluxes. Obviously, gross air–water exchange fluxes are significantly higher than net fluxes.

The total wet deposition of PCBs and PCDD/Fs to the Atlantic Ocean is on the order of 4100 and 2500  $\text{kg yr}^{-1}$ , respectively. The first estimation is about 1 order of magnitude lower than a pioneering estimate made by Duce et al. (54). Presumably, Duce et al. (54) obtained higher fluxes due to significantly higher PCB concentrations a decade ago and limited availability of spatially resolved data. On the other hand, the estimate of total PCDD/F wet deposition fluxes is higher than the value of 900 ( $\pm 300$ )  $\text{kg yr}^{-1}$  estimated by the study of Baker and Hites (55), based on measurement in the Barbados/Bermudas, thus not considering spatial variability. This was also based on aerosol measurements after long-range transport across the Atlantic Ocean, thereby representing lower case estimates (as the air masses had been subject to deposition and degradation events).

Wet deposition is estimated to be 2–5-fold the dry deposition fluxes to the Atlantic (2200  $\text{kg yr}^{-1}$  for PCBs and 500  $\text{kg yr}^{-1}$  for PCDD/Fs), consistent with other studies that report wet deposition exceeding dry aerosol deposition fluxes in many assessments at local scale (36, 56–58) (Table 2). A similar dominance of the wet over the dry aerosol deposition was also suggested by Baker and Hites (900 vs 200  $\text{kg/year}$ ) for PCDD/Fs on a global scale (55). Finally, net air–water exchange fluxes to the Atlantic Ocean are estimated to be 22 000  $\text{kg yr}^{-1}$  for PCBs and 1300  $\text{kg yr}^{-1}$  for PCDD/Fs. It should be remembered that estimations of wet deposition fluxes described here are dependent on the various assumptions used in the calculations such as values of  $H$ ,  $W_P$ ,  $K_P$ , etc. The uncertainty associated with these estimations is assessed by a comprehensive comparison with available field studies in the following section.

**Comparison with Direct Measurements of Wet Deposition Fluxes.** A comprehensive validation of wet deposition fluxes is not possible because there is a lack of available measurements in oceanic areas. Furthermore, measurements often refer to bulk deposition (dry + wet), because of the sampling devices used. We are therefore compelled to use measurements performed in coastal areas, islands, or lakes.

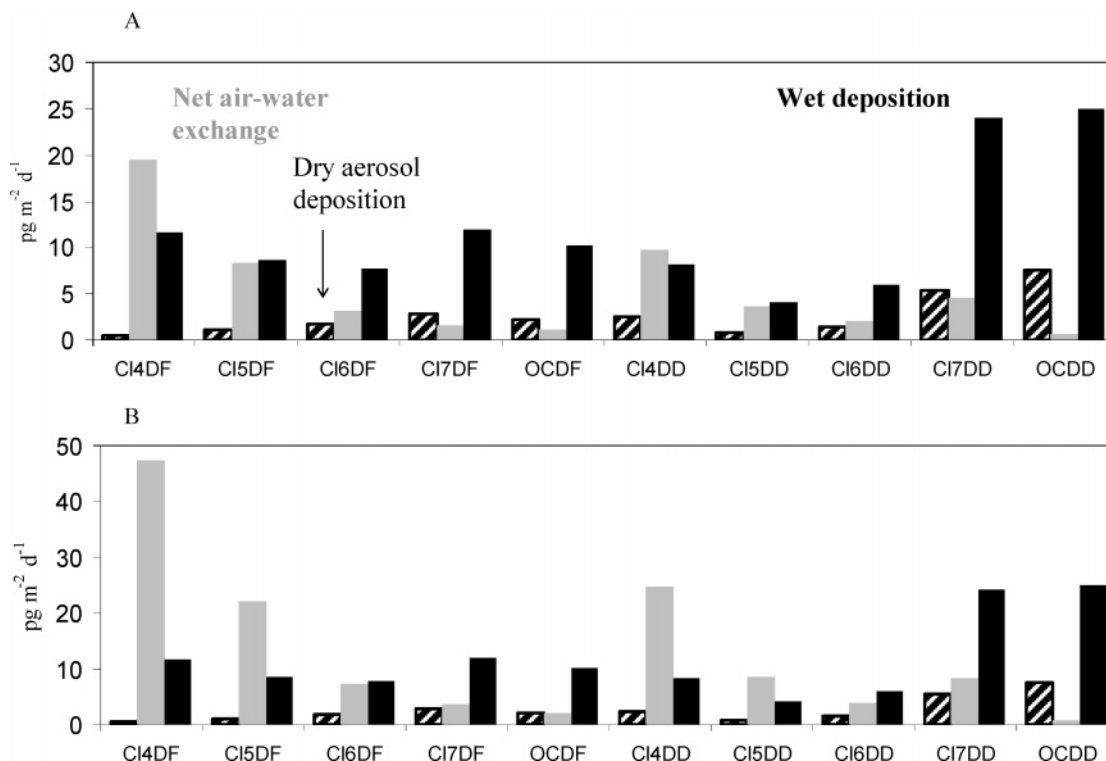


**FIGURE 5.** Comparison of mean dry aerosol deposition, net air–water exchange, and wet deposition fluxes for PCDD/Fs homologue groups (A) and PCBs (B) for the Atlantic Ocean.

**TABLE 2. Comparison between Wet Deposition Coastal Fluxes Measured in the Field and Estimated in This Study<sup>a</sup>**

source	location name	(latitude, longitude)	year of sampling	type of environment	measd $F_{WD}$ $\Sigma PCBs$ [ng $m^{-2} yr^{-1}$ ] <sup>b</sup>	modeled $F_{WD} \Sigma PCBs$ [ng $m^{-2} yr^{-1}$ ] <sup>c</sup>	modeled $F_{WD} \Sigma PCBs$ [ng $m^{-2} yr^{-1}$ ] <sup>d</sup>
Van Ry (36)	Tuckerton, U.S.	(39 N, 74 W)	2000–2001	coastal, light residential	268 (310)	870	130
Mandalakis et al. (64)	Crete Island, eastern Mediterranean	(35 N, 25 E)	2000–2001	marine background	(820)	71	107
Van Drooge (56)	Izaña, Tenerife, NE Atlantic	(28 N, 16 E)	1999–2000	subtropical island, free troposphere	735 (1300)	356	706
Park et al. (65)	Galveston Bay, TX	(29 N, 95 W)	1995–1996	coastal, urban influenced	(1530)	3200	3600
Brorström-Lundén and Lögfrén (66)	Lake Gardsjön, Swedish west coast	(59 N, 11 E)	1991–1994	rural	1168	340	

<sup>a</sup> Reported wet deposition fluxes measured by wet only sampler, bulk when sampler collects dry + wet. Values in parentheses refer to all the PCBs congeners, not just those studied in the paper. <sup>b</sup> Or bulk flux. <sup>c</sup> Measured  $C_G$  and  $C_P$  derived theoretically. <sup>d</sup> Measured  $C_G$  and  $C_P$ .

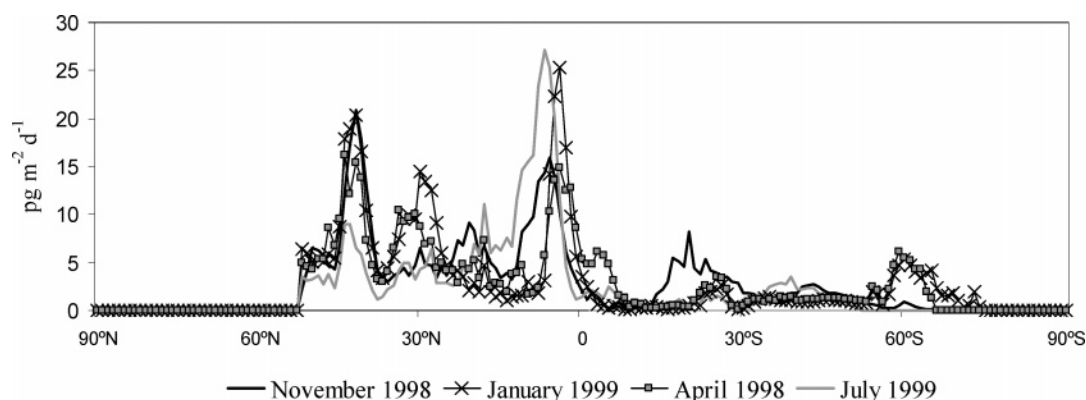


**FIGURE 6. Estimated wet deposition fluxes for Cl<sub>5</sub>DDs for January, April, July, and November 1998–1999.**

For PCDD/Fs, the lack of measurements over oceans and in coastal areas is even more acute, thus inland measurements have been used.

Average wet deposition fluxes estimated for the whole Atlantic Ocean in this study (43 and 110 ng m<sup>-2</sup> yr<sup>-1</sup> for  $\Sigma PCDD/Fs$  and  $\Sigma PCB$ , respectively) are lower than all the values reported in other studies (see Table 2). This is because higher fluxes are generally observed close to source areas rather than in remote oceanic regions. Validation ideally must be done by comparing the reported values with those estimated in the same region. To this end, a validation of our estimations has been carried out by estimating wet deposition fluxes in a window of 5° × 5° around the reported oceanic or coastal sampling sites, using the gas-phase concentrations reported in the respective reference. This exercise gave estimates within a factor 2–3 of the measured wet fluxes, with the best agreement obtained where measurements were carried in remote oceanic regions, such as in Tenerife Island in the subtropical eastern Atlantic (56) (see Table 2). The modeled estimates were even better if the reported particle-phase concentrations are used. Indeed, estimates of PCB wet deposition fluxes were 710 ng m<sup>-2</sup> yr<sup>-1</sup> for the subtropical eastern Atlantic, compared to measurements of 735 ng m<sup>-2</sup> yr<sup>-1</sup> (56). Similarly, estimates in the western north Atlantic were 130 ng m<sup>-2</sup> yr<sup>-1</sup>, compared to measurements of 270 ng m<sup>-2</sup> yr<sup>-1</sup> (36).

In summary, the modeled values derived here appear to reasonably represent the atmospheric deposition to most oceanic regions. Furthermore, the trend in the homologue profile of depositional fluxes is similar to that of other studies, particularly those on PCDD/Fs (10, 59, 60). Discrepancies tend to be greater when considering continental coastal locations instead of islands. This may be linked to the uncertainties of satellites to retrieve coastal values and

because many coastal locations are impacted by urban areas. On the other hand, agreement for PCBs with the wet deposition flux improve if measured particle concentration are used, reflecting the difficulties of representing  $C_P$  from  $K_P$  values. Finally, the fact that the model sometimes gives underestimates and sometimes gives overestimates compared to direct measurements show that there is no systematic bias in the methodology used to derive these global wet deposition fluxes.

**Seasonal Trends of Wet Deposition Fluxes.** To observe the effects of the seasonality of some meteorological parameters such as precipitation patterns, temperature and TSP, the latitudinal distribution of wet deposition fluxes over the Atlantic Ocean for four seasonally representative months has been estimated for Cl<sub>5</sub>DD (see Figure 6), assuming that Cl<sub>5</sub>DD gas concentrations are constant throughout the year (2, 15, 61). Conversely, aerosol-phase PCDD/F concentrations have been estimated from temperature-dependent  $K_P$  values. Major scavenging fluxes are found in the Northern Hemisphere, where seasonal variability tends to be greater. Seasonality observed in temperate regions is mainly driven by the variable temperatures. Lower temperatures, characteristic of hemispheric winter, increase the fraction of atmospheric POPs bound to aerosols, thus increasing the overall scavenging. Furthermore, raised levels of wet deposition fluxes along the ITCZ are clearly marked, and they are linked to the northward shift and intensification of the ITCZ and during June–August. Interannual variability (not assessed) may be mainly affected by the El Niño–Southern Oscillation (ENSO) (62).

**Dominant Atmospheric Deposition Flux to the Global Ocean.** In addition to the comparison of the different depositional processes for the Atlantic Ocean, it is of interest to determine the dominant deposition process for the global



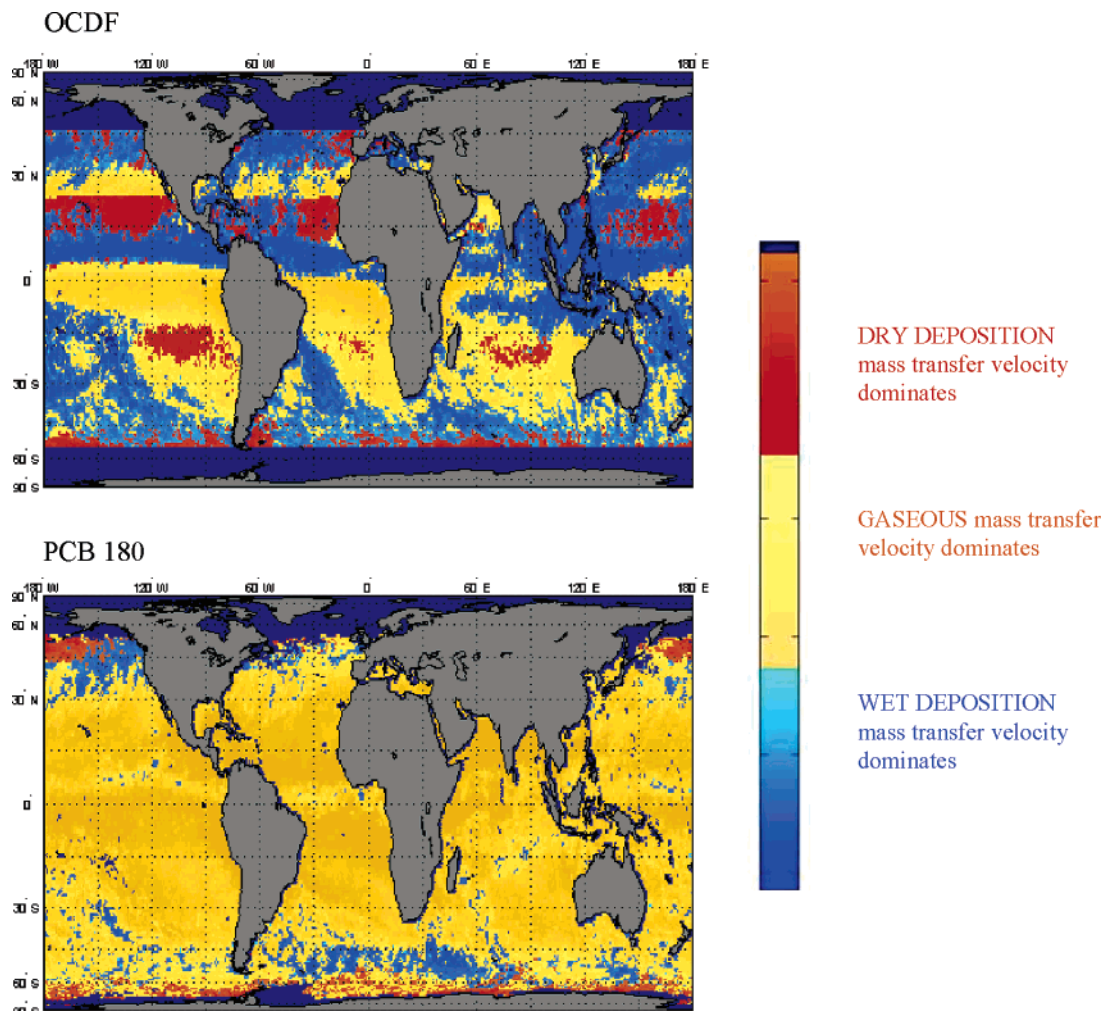


FIGURE 7. Dominant mass transfer velocity for OCDF and PCB 180.

oceans with a spatial resolution that allows differentiation among different regions. Since field measurements are not available for most oceans, this comparison should be independent of POP atmospheric concentrations. Comparisons can be performed by considering the mass transfer coefficients. Gaseous absorption to the surface ocean and wet and dry deposition fluxes are depositional processes behaving in parallel. Thus, the dominant depositional flux will be that with greater mass transfer coefficient, independent of the aerosol- and gas-phase concentrations of the compounds (15).

The mass transfer coefficient for wet deposition is given by  $(W_G + (W_p\phi/(1-\phi))p_0)$  (from eq 15). The absorption flux is given by  $(k_{AW,rain}/H')f + (k_{AW}/H')(1-f)$  (from eq 16). Dry aerosol deposition is related to particle phase concentrations, so  $v_D$  cannot be compared directly to the previous mass transfer velocities (see eq 17). The dry aerosol deposition flux needs to be related to the gas-phase concentration, by using gas-particle partitioning models. Reordering eq 18 gives

$$F_{DD} = v_D \frac{\phi}{1-\phi} C_G \quad (18)$$

Therefore, the mass transfer coefficient for dry deposition is given by  $(v_D\phi)/(1-\phi)$ .

Figure 7 shows the dominant depositional mechanism at the global scale for two high chlorinated POPs: OCDF and PCB 180. Because of the high degree of chlorination, processes favored by particle-phase sorption (dry aerosol deposition,

particle wet deposition) have a greater importance than for other POPs. PCBs, which are found mainly in the gas phase, are primarily introduced into the ocean water surface by gaseous absorption almost everywhere. This trend may reverse at high latitudes; where the low temperatures and the high concentrations of marine aerosol induce an increased fraction of contaminant bound to particles (15) and thus the dominance of dry or wet deposition.

PCDD/Fs show a higher affinity to aerosols, presumably due to adsorption to aerosol soot carbon (63). Hence, for these compounds, either wet or dry deposition is the dominant process in some oceanic regions, which can be a significant fraction of the oceans for the more hydrophobic chemicals (OCDF). Dry aerosol deposition may become dominant between 10 and 25° N in the Atlantic due to Saharan-Sahel dust plumes and oceanic areas of the mid-high Southern Hemisphere, where there are higher loadings of sea salt. By contrast, dominance of wet deposition fluxes is clearly marked downwind of continents in the mid latitudes (east coasts) and in the tropics.

### Acknowledgments

The remote sensing data used in this study were acquired as part of the NASA's Earth Science Enterprise. The algorithms behind the level 3 products were developed by the MODIS Science Teams. The data were processed by the MODIS Adaptive Processing System (MODAPS) and Goddard Distributed Active Archive Center (DAAC, <http://www.daac.ornl.gov>) and are archived and distributed by the Goddard DAAC. NOAA and ATSR processing teams are also



acknowledged. The authors appreciate useful comments made by Santiago Gassó (NASA) and David Ho (Columbia University, NY). This work was supported by the Spanish Ministry of Science and Technology through Project AMIGOS (REN2001-3462/CLI).

### Supporting Information Available

Further details on methodology to estimate gas-phase washout due to adsorption on the raindrop is found in Annex I. Comparison of gross absorption and wet deposition fluxes is given in Annex II. This material is available free of charge via the Internet at <http://pubs.acs.org>.

### Literature Cited

- Poster, D. L.; Baker, J. E. Mechanisms of atmospheric wet deposition of chemical contaminants. In *Atmospheric Deposition of Contaminants to the Great Lakes and Coastal Waters*; Baker, J. E., Ed.; Proceedings from a session at the SETAC 15th Annual Meeting October 30–November 4, 1994; SETAC Press: Denver, 1994; pp 51–72.
- Wania, F.; Axelman, J.; Broman, D. A review of processes involved in the exchange of persistent organic pollutants across the air–sea interface. *Environ. Pollut.* **1998**, *102*, 3–23.
- Schulz-Bull, D. E.; Petrick, G.; Bruhn, R.; Duinker, J. C. Chlorobiphenyls (PCB) and PAHs in water masses of the northern North Atlantic. *Mar. Chem.* **1998**, *61*, 101–114.
- Shatalov, V.; Dutchak, S.; Fedyunin, M.; Mantseva, E.; Strukov, B.; Varygina, M.; Vulykh, N.; Aas, W.; Mano, S. Persistent Organic Pollutants in the Environment. EMEP Status Report 3/2003; 2003.
- Jones, K. C.; de Voogt, P. Persistent organic pollutants (POPs): State of the science. *Environ. Pollut.* **1999**, *100*, 209–221.
- Wania, F.; Daly, G. L. Estimating the contribution of degradation in air and deposition to the deep sea to the global loss of PCBs. *Atmos. Environ.* **2002**, *36*, 5581–5593.
- Dachs, J.; Bayona, J. M.; Venugopalan, I.; Albaigés, J. Monsoon-driven vertical fluxes of organic pollutants in the western Arabian Sea. *Environ. Sci. Technol.* **1999**, *33*, 3949–3956.
- Pankow, J. F. An absorption model of gas/particle partitioning of organic compounds in the atmosphere. *Atmos. Environ.* **1994**, *28*, 185–188.
- Bidleman, T. Atmospheric processes. *Environ. Sci. Technol.* **1988**, *22*, 361–367.
- Eitzer, B. D.; Hites, R. A. Atmospheric transport and deposition of polychlorinated dibenzo-*p*-dioxins and dibenzofurans. *Environ. Sci. Technol.* **1989**, *23*, 1396–1401.
- Harman-Fetchco, J. A.; McConnell, L. L.; Rice, C. P.; Baker, J. E. Wet deposition and air–water exchange of currently used pesticides to a subestuary of the Chesapeake Bay. *Environ. Sci. Technol.* **2000**, *34*, 1462–1498.
- Ho, D. T.; Bliven, L. F.; Wanninkhof, R.; Schlosser, P. The effect of rain on air–water gas exchange. *Tellus* **1997**, *49B*, 149–158.
- Ho, D. T.; Zappa, C. J.; McGillis, W. R.; Bliven, L. F.; Ward, B.; Dacey, J. W. H.; Schlosser, P.; Hendricks, M. B. Influence of rain on air–sea gas exchange: Lessons from a model ocean. *J. Geophys. Res.* **2004**, *109*, C08S18.
- Simcik, M. F. The importance of surface adsorption on the washout of semivolatile organic compounds by rain. *Atmos. Environ.* **2004**, *38*, 491–501.
- Jurado, E.; Jaward, F. M.; Lohmann, R.; Jones, K. C.; Simó, R.; Dachs, J. Atmospheric dry deposition of persistent organic pollutants to the Atlantic and inferences for the global oceans. *Environ. Sci. Technol.* **2004**, *38*, 5505–5513.
- Lohmann, R.; Ockenden, W. A.; Shears, J.; Jones, K. C. Atmospheric distribution of polychlorinated dibenzo-*p*-dioxins, dibenzofurans (PCDD/Fs), and non-ortho biphenyls (PCBs) along a north–south transect. *Environ. Sci. Technol.* **2001**, *35*, 4046–4053.
- Jaward, F. M.; Barber, J. L.; Booij, K.; Dachs, J.; Lohmann, R.; Jones, K. C. Evidence for dynamic air–water coupling and cycling of persistent organic pollutants over the open Atlantic Ocean. *Environ. Sci. Technol.* **2004**, *38*, 2617–2625.
- Dachs, J.; Lohmann, R.; Ockenden, W. A.; Méjanelle, L.; Eisenreich, S. J.; Jones, K. C. Oceanic biogeochemical controls on global dynamics of persistent organic pollutants. *Environ. Sci. Technol.* **2002**, *36*, 4229–4237.
- Totten, L. A.; Brunciak, P. A.; Gigliotti, C. L.; Dachs, J.; Glenn, T. R.; Nelson, E. D.; Eisenreich, S. J. Dynamic air–water exchange of polychlorinated biphenyls in the New York–New Jersey Harbor estuary. *Environ. Sci. Technol.* **2001**, *35*, 3834–3840.
- Dachs, J.; Eisenreich, S. J.; Baker, J. E.; Ko, F.-C.; Jeremiason, J. D. Coupling of phytoplankton uptake and air–water exchange of persistent organic pollutants. *Environ. Sci. Technol.* **1999**, *33*, 3653–3660.
- Bauer, P.; Mahfouf, J.-F. GEWEX-GPCP Workshop on Objective Analysis of Precipitation, 2003.
- Ferraro, R. R. Special sensor microwave imager derived global rainfall estimates for climatological applications. *J. Geophys. Res.* **1997**, *102*, 16715–16735.
- Ligocki, M. P.; Leuenberger, C.; Pankow, J. F. Trace of organic compounds in rain. III. Particle Scavenging of neutral organic compounds. *Atmos. Environ.* **1985**, *19*, 1619–1626.
- Harner, T.; Bidleman, T. Octanol–air partition coefficient for describing particle–gas partitioning of aromatic compounds in urban air. *Environ. Sci. Technol.* **1998**, *32*, 1494–1502.
- Dachs, J.; Eisenreich, S. J. Adsorption onto aerosol soot carbon dominates gas–particle partitioning of polycyclic aromatic hydrocarbons. *Environ. Sci. Technol.* **2000**, *34*, 3690–3697.
- Gassó, S.; Hegg, D. A. On the retrieval of columnar aerosol mass and CCN concentration by MODIS. *J. Geophys. Res.* **2003**, *108*, 4010–4035.
- Ligocki, M. P.; Leuenberger, C.; Pankow, J. F. Trace of organic compounds in rain. II. Gas Scavenging of neutral organic compounds. *Atmos. Environ.* **1985**, *19*, 1609–1617.
- Dickhut, R. M.; Gustafson, K. E. Atmospheric washout of polycyclic aromatic hydrocarbons in the southern Chesapeake Bay Region. *Environ. Sci. Technol.* **1995**, *29*, 1518–1525.
- Poster, D. L.; Baker, J. E. Influence of submicron particles on Hydrophobic organic contaminants in precipitation. 2. Scavenging of polycyclic aromatic hydrocarbons by rain. *Environ. Sci. Technol.* **1996**, *30*, 349–354.
- Roth, C. M.; Goss, K.-U.; Schwarzenbach, R. P. Adsorption of a diverse set of organic vapors on the bulk water surface. *J. Colloid Interface Sci.* **2002**, *252*, 21–30.
- Marshall, J. S.; Palmer, W. M. The distribution of the raindrops with size. *J. Meteorol.* **1948**, *5*, 165–166.
- Brunner, S.; Hornung, E.; Santi, H.; Woiff, E.; Piringer, O. G. Henry's law constants for polychlorinated biphenyls: experimental determination and structure–property relationships. *Environ. Sci. Technol.* **1990**, *24*, 1751–1754.
- Bamford, H. A.; Poster, D. L.; Baker, J. E. Henry's law constants of polychlorinated biphenyl congeners and their variation with temperature. *J. Chem. Eng. Data* **2000**, *45*, 1069–1074.
- Dunnivant, F. M.; Elzerman, A. W.; Jurs, P. C.; Hasan, M. N. Quantitative structure–property relationships for aqueous solubilities and Henry law constants of polychlorinated biphenyls. *Environ. Sci. Technol.* **1992**, *26*, 1567–1573.
- Koester, C. J.; Hites, R. A. Wet and dry deposition of chlorinated dioxins and furans. *Environ. Sci. Technol.* **1992**, *26*, 1375–1382.
- Van Ry, D. A.; Gigliotti, C. L.; Glenn, T. R.; Nelson, E. D.; Totten, L. A.; Eisenreich, S. J. Wet deposition of polychlorinated biphenyls in urban and background areas of the Mid-Atlantic States. *Environ. Sci. Technol.* **2002**, *36*, 3201–3209.
- Franz, T. P.; Eisenreich, S. J. Snow scavenging of polychlorinated biphenyls and polycyclic aromatic hydrocarbons in Minnesota. *Environ. Sci. Technol.* **1998**, *32*, 1771–1778.
- Offenberg, J. H.; Baker, J. E. Precipitation scavenging of polychlorinated biphenyls and polycyclic aromatic hydrocarbons along an urban to over-water transect. *Environ. Sci. Technol.* **2002**, *36*, 3763–3771.
- Poster, D. L.; Baker, J. E. Influence of submicron particles on Hydrophobic organic contaminants in precipitation. 1. Concentrations and distributions of polycyclic aromatic hydrocarbons and polychlorinated biphenyls in rainwater. *Environ. Sci. Technol.* **1996**, *30*, 341–348.
- Radke, L. F.; Hobbs, P. V.; Eltgroth, M. W. Scavenging of aerosol particles by precipitation. *J. Appl. Meteorol.* **1980**, *19*, 715–722.
- Mircea, M.; Stefan, S.; Fuzzi, S. Precipitation scavenging coefficient: influence of measured aerosol and raindrop size distributions. *Atmos. Environ.* **2000**, *34*, 5169–5174.
- Nicholson, K. W.; Branson, J. R.; Giess, P. Field measurements of the below-cloud scavenging of particulate material. *Atmos. Environ.* **1991**, *25A*, 771–777.
- Mackay, D.; Paterson, S.; Schroeder, W. H. Model describing the rates of transfer processes of organic chemicals between atmosphere and water. *Environ. Sci. Technol.* **1986**, *20*, 0.
- Schwarzenbach, R. P.; Gschwend, P. M.; Imboden, D. M. *Environmental Organic Chemistry*, 2nd ed.; Wiley-Interscience: New York, 2000.

- (45) Bruhn, R.; Lakaschus, S.; McLachlan, M. S. Air/sea gas exchange of PCBs in the southern Baltic Sea. *Atmos. Environ.* **2003**, *37*, 3445–3454.
- (46) Wanninkhof, R.; McGillis, W. R. A cubic relationship between air-sea CO<sub>2</sub> exchange and wind speed. *Geophys. Res. Lett.* **1999**, *26*, 1889–1892.
- (47) Nightingale, P. D.; Malin, G.; Law, C. S.; Watson, A. J.; Liss, P. S.; Liddicoat, M. I.; Boutin, J.; Upstill-Goddard, R. C. In situ evaluation of air-sea gas exchange parameterizations using novel conservative and volatile tracers. *Global Biogeochem. Cycles* **2000**, *14*, 373–387.
- (48) Nightingale, P. D.; Liss, P. S.; Schlosser, P. Measurements of air-sea gas transfer during an open ocean algal bloom. *Geophys. Res. Lett.* **2000**, *27*, 2117–2120.
- (49) Pérez, S.; Dachs, J.; Barceló, D. Sea breeze modulated volatilization of polycyclic aromatic hydrocarbons from the Masnou Harbor (NW Mediterranean Sea). *Environ. Sci. Technol.* **2003**, *37*, 3794–3802.
- (50) Livingstone, D. M.; Imboden, D. M. The non-linear influence of wind-speed variability on gas transfer in lakes. *Tellus* **1993**, *45B*, 275–295.
- (51) Wilks, D. S.; Wilby, R. L. The weather generation game: A review of stochastic weather models. *Prog. Phys. Geogr.* **1999**, *23*, 329–357.
- (52) Ho, D. T.; Asher, W. E.; Bliven, L. F.; Schlosser, P.; Gordan, E. L. On mechanisms of rain-induced air-water gas exchange. *J. Geophys. Res.* **2000**, *105*, 24045–24057.
- (53) Franz, T. P.; Eisenreich, S. J. Wet deposition of polychlorinated biphenyls to Green Bay, Lake Michigan. *Chemosphere* **1993**, *26*, 1767–1788.
- (54) Duce, R. A.; Liss, P. S.; Merrill, J. T.; Atlas, E. L.; Buat-Menard, P.; Hicks, B. B.; Miller, J. M.; Prospero, J. M.; Arimoto, R.; Church, T. M.; Ellis, W.; Galloway, J. N.; Hansen, L.; Jickells, T. D.; Knap, A. H.; Reinhardt, K. H.; Schneider, B.; Soudine, A.; Tokos, J. J.; Tsunogai, S.; Wollast, R.; Zhou, M. The atmospheric input of trace species to the world ocean. *Global Biogeochem. Cycles* **1991**, *5*, 193–259.
- (55) Baker, J. I.; Hites, R. A. Polychlorinated dibenzo-*p*-dioxins and dibenzofurans in the remote North Atlantic marine atmosphere. *Environ. Sci. Technol.* **1999**, *33*, 14–20.
- (56) Van Drooge, B. L.; Grimalt, J. O.; Torres-Garcia, C. J.; Cuevas, E. Deposition of semi-volatile organochlorine compounds in the free troposphere of the eastern north Atlantic Ocean. *Mar. Pollut. Bull.* **2001**, *42*, 628–634.
- (57) Eisenreich, S. J.; Strachan, W. M. J. Estimating atmospheric deposition of toxic substances to the Great Lakes. Canada Centre for Inland Waters: 1992.
- (58) Swackhamer, D. L.; McVeety, B. D.; Hites, R. A. Deposition and evaporation of polychlorobiphenyl congeners to and from Siskiwit Lake, Isle Royale, Lake Superior. *Environ. Sci. Technol.* **1988**, *22*, 664–672.
- (59) Ogura, I.; Masunaga, S.; Nakanishi, J. Analysis of atmospheric behavior of PCDDs/PCDFs by a one-compartment box model. *Chemosphere* **2003**, *53*, 399–412.
- (60) Schröder, J.; Welsch-Pausch, K.; McLachlan, M. S. Measurement of atmospheric deposition of polychlorinated dibenzo-*p*-dioxins (PCDDs) and dibenzofurans (PCDFs) to a soil. *Atmos. Environ.* **1997**, *31*, 2983–2989.
- (61) Van Drooge, B. L.; Grimalt, J. O.; Torres-Garcia, C. J.; Cuevas, E. Semivolatile organochlorine compounds in the free troposphere of the Northeastern Atlantic. *Environ. Sci. Technol.* **2002**, *36*, 1155–1161.
- (62) Guelle, W.; Balkanski, Y. J.; Schulz, M.; Dulac, F.; Monfray, P. Wet deposition in a global size-dependent aerosol transport model. 1. Comparison of 1 year 210Pb simulation with ground measurements. *J. Geophys. Res.* **1998**, *103*, 11429–11445.
- (63) Lohmann, R.; Harner, T.; Thomas, G. O.; Jones, K. C. A comparative Study of the Gas-Particle partitioning of PCDD/Fs, PCBs, and PAHs. *Environ. Sci. Technol.* **2000**, *34*, 4943–4951.
- (64) Mandalakis, M.; Stephanou, E. G. Wet deposition of polychlorinated biphenyls in the eastern Mediterranean. *Environ. Sci. Technol.* **2004**, *38*, 3011–3018.
- (65) Park, J.-S.; Wade, T. L.; Sweet, S. Atmospheric deposition of organochlorine contaminants to Galveston Bay, Texas. *Atmos. Environ.* **2001**, *35*, 3315–3324.
- (66) Brorström-Lundén, E.; Löfgren, C. Atmospheric fluxes of persistent semivolatile organic pollutants to a forest ecological system at the Swedish west coast and accumulation in spruce needles. *Environ. Pollut.* **1998**, *102*, 139–149.

Received for review September 9, 2004. Revised manuscript received December 11, 2004. Accepted December 16, 2004.

ES048599G